# IPP Garching Contributions to the Application and Development of the non-linear MHD code JOREK

Matthias Hölzl

# Overview

- Non-linear MHD code
- Divertor tokamaks including X-point(s)
- Focus on plasma edge simulations
- Originally developed by Guido Huysmans at CEA Cadarache Huysmans and Czarny [2007]
- Reduced MHD in toroidal geometry (next slide)
- Other models:
  - Two-fluid extensions (M. Becoulet, S. Pamela)
  - Neutrals (C. Reux)
  - Full MHD
- Fortran 90/95
- MPI + OpenMP parallelized

# Reduced MHD Equations

$$\frac{\partial \Psi}{\partial t} = \eta j - R\,[u, \Psi] - F_0 \frac{\partial u}{\partial \phi}$$

$$\frac{\partial \rho}{\partial t} = -\nabla \cdot (\rho \mathbf{v}) + \nabla \cdot (D_\perp \nabla_\perp\, \rho) + S_\rho$$

$$\frac{\partial (\rho T)}{\partial t} = -\mathbf{v} \cdot \nabla (\rho T) - \gamma \rho T \nabla \cdot \mathbf{v} + \nabla \cdot \left( K_\perp \nabla_\perp\, T + K_{||} \nabla_{||} T \right) + S_T$$

$$\mathbf{e}_\phi \cdot \nabla \times \left\{ \rho \frac{\partial \mathbf{v}}{\partial t} = -\rho (\mathbf{v} \cdot \nabla) \mathbf{v} - \nabla p + \mathbf{j} \times \mathbf{B} + \mu \Delta \mathbf{v} \right\}$$

$$\mathbf{B} \cdot \left\{ \rho \frac{\partial \mathbf{v}}{\partial t} = -\rho (\mathbf{v} \cdot \nabla) \mathbf{v} - \nabla p + \mathbf{j} \times \mathbf{B} + \mu \Delta \mathbf{v} \right\}$$

$$j \equiv -j_\phi = \Delta^* \Psi$$

$$\omega \equiv -\omega_\phi = \nabla^2_{pol}\, u$$

Variables: $\Psi$, $u$, $j$, $\omega$, $\rho$, $T$, $v_{||}$

Ideal wall + Bohm boundary conditions

Definitions: $\mathbf{B} = \frac{F_0}{R} \mathbf{e}_\phi + \frac{1}{R} \nabla \Psi \times \mathbf{e}_\phi$ and $\mathbf{v} = -R \nabla u \times \mathbf{e}_\phi + v_{||} \mathbf{B}$

# Typical code run

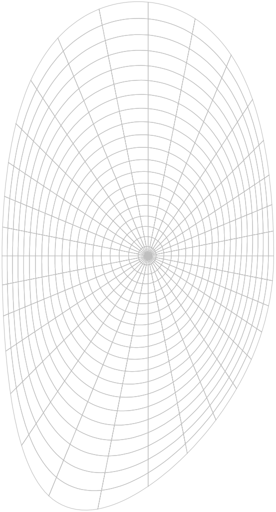

- Initial grid (Grids shown with reduced resolution)
- Equilibrium data ($F_0$, $\Psi_{\text{bnd}}$, profiles for $T$, $\rho$, $FF'$)
- Grad-Shafranov
- Flux aligned grid (may include X-points)
- Radial and poloidal grid meshing
- Grad-Shafranov
- Axisymmetric flows
- Time-integration
- Analysis of restart-files:
  - Poincare plots
  - 2D or 3D VTK files
  - ...

# Typical code run

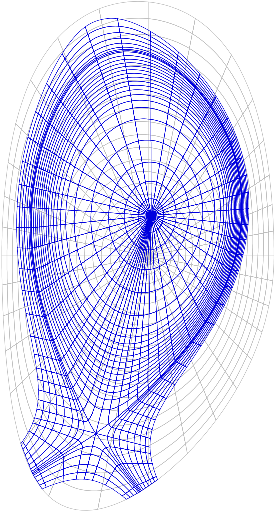

- Initial grid (Grids shown with reduced resolution)
- Equilibrium data ($F_0$, $\Psi_{\text{bnd}}$, profiles for $T$, $\rho$, $FF'$)
- Grad-Shafranov
- Flux aligned grid (may include X-points)
- Radial and poloidal grid meshing
- Grad-Shafranov
- Axisymmetric flows
- Time-integration
- Analysis of restart-files:
  - Poincare plots
  - 2D or 3D VTK files
  - ...

# Typical code run

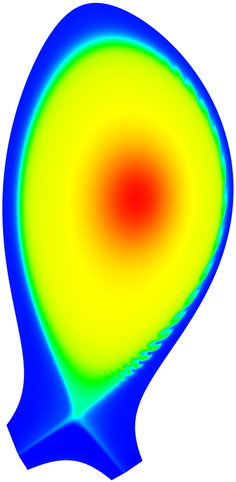

- Initial grid (Grids shown with reduced resolution)
- Equilibrium data ($F_0$, $\Psi_{\text{bnd}}$, profiles for $T$, $\rho$, $FF'$)
- Grad-Shafranov
- Flux aligned grid (may include X-points)
- Radial and poloidal grid meshing
- Grad-Shafranov
- Axisymmetric flows
- Time-integration
- Analysis of restart-files:
    - Poincare plots
    - 2D or 3D VTK files
    - ...

# Monitor a running simulation

- Script plot_live_data.sh using gnuplot
- Allows to plot some data while a simulation is running
- Non-regression testing partly uses this infrastructure Latu et al. [2012]
- For instance, energy time-traces:

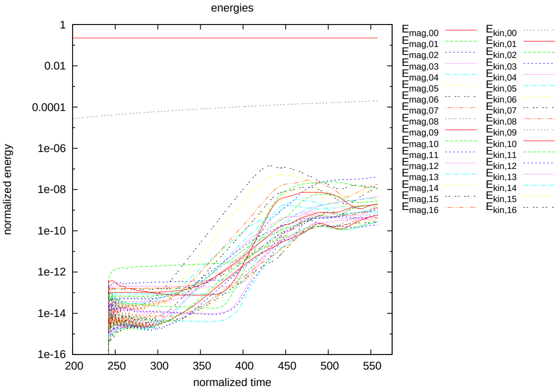


(Hard to continue simulation into non-linear phase)

# Synthetic Magnetics (R.Wenninger)

- Remove ideal-wall boundary conditions from solution in post-processing
- Add effects of AUG conducting structures
- Generate synthetic Mirnov-coil signals

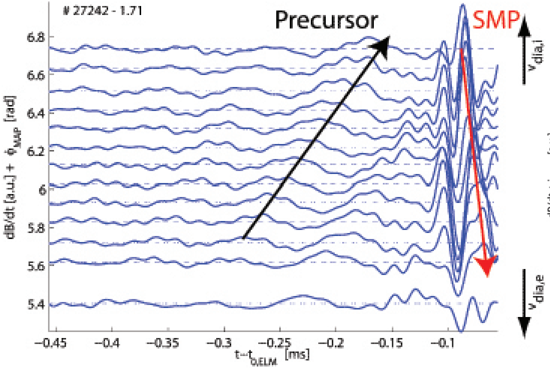


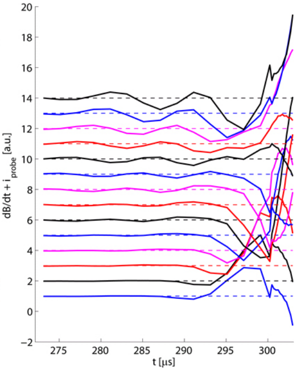

# 2D Fourier analysis

- Determine straight field line coordinates
- 2D Fourier analysis in these coordinates

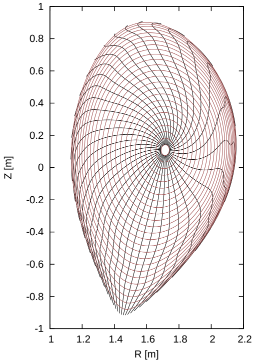


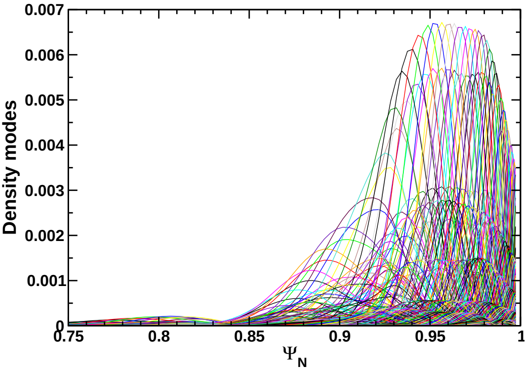

# Additional postprocessing

- Run `jorek2_postproc` with simple script or interactively
- For example, density at outboard midplane and flux-suface averaged density:

```
namelist input1                                         # load input namelist
set linepoints 150                                      # set number of points
for step 480 to 500 do                                  # loop over time-steps
  line density psi_n 2.00 0.11 0 2.19 0.11 0  # values along straight line
  average density                                       # flux-surface average
done
```

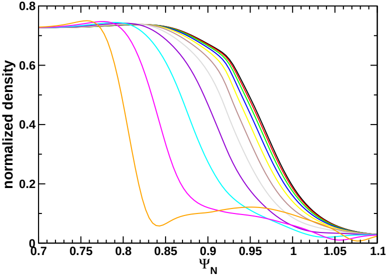


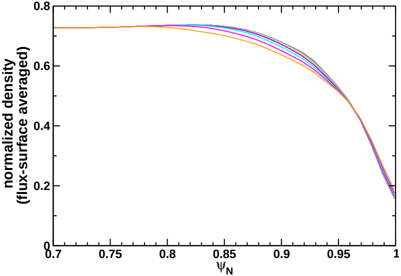

# Overview

## Simulations performed

- Edge Localized Modes (ELMs) in realistic ASDEX Upgrade geometry
- Focus on early phase until non-linear saturation starts
- Comparably high number of toroidal modes
  - Periodicity 1: $n = 0, 1, 2, \ldots 16$
  - Periodicity 2: $n = 0, 2, 4, \ldots 16$
  - ...

## Questions addressed

- Spatial mode structure?
- Non-linear effects?
- Mode saturation?

# Input Profiles

- Input profiles taken from typical ASDEX Upgrade discharge:

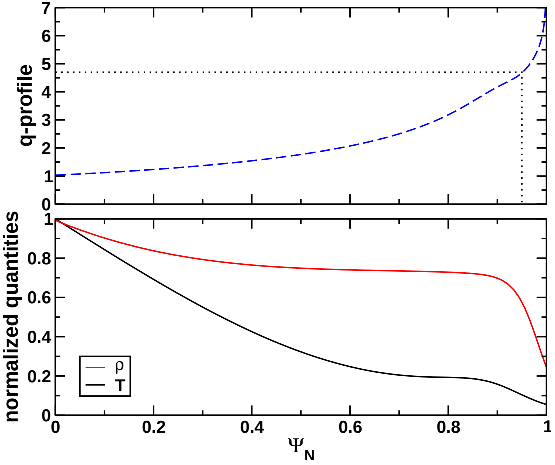

# Flux-algined X-point Grid

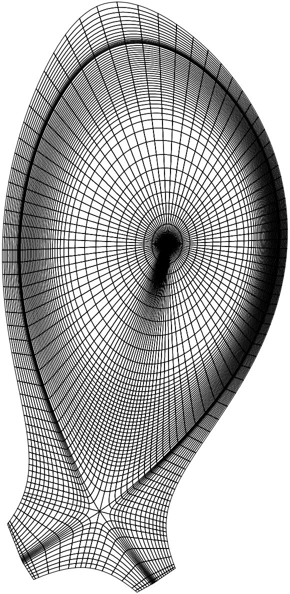

# Ballooning Structure

- Mode-coupling causes localization of ballooning-filaments:

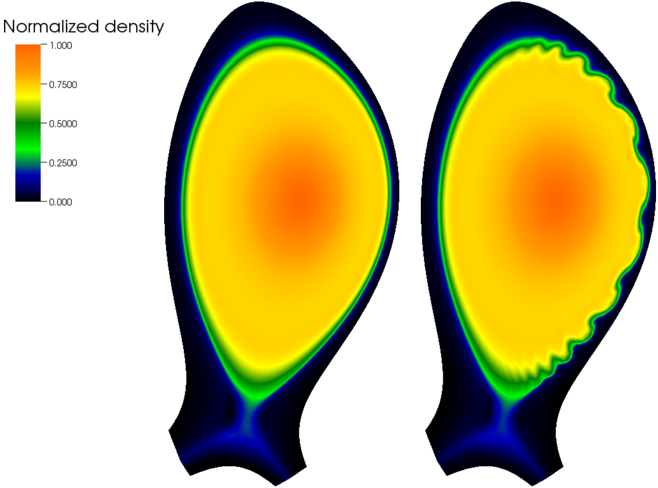


unperturbed $\qquad n = 0, 8, 16$

# Ballooning Structure

- Mode-coupling causes localization of ballooning-filaments:

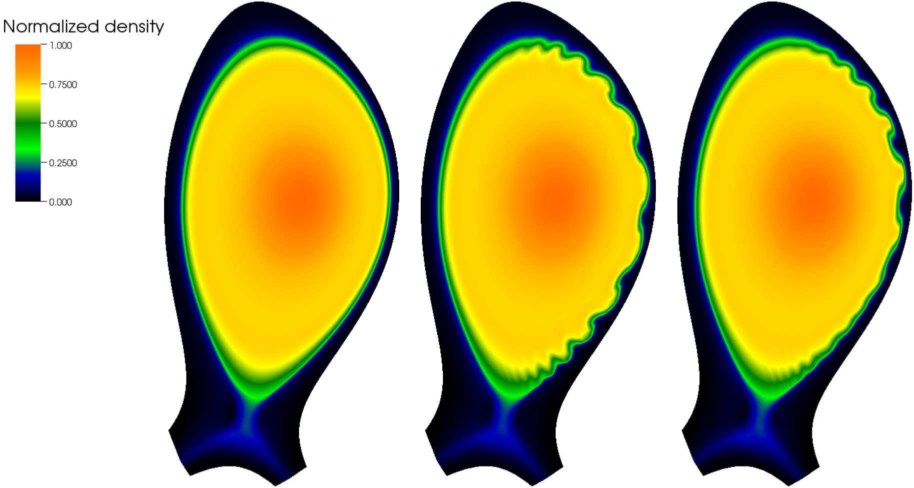


unperturbed $\qquad n = 0, 8, 16 \qquad n = 0, 1, 2, \ldots, 16$

## Poloidal Flux Perturbation

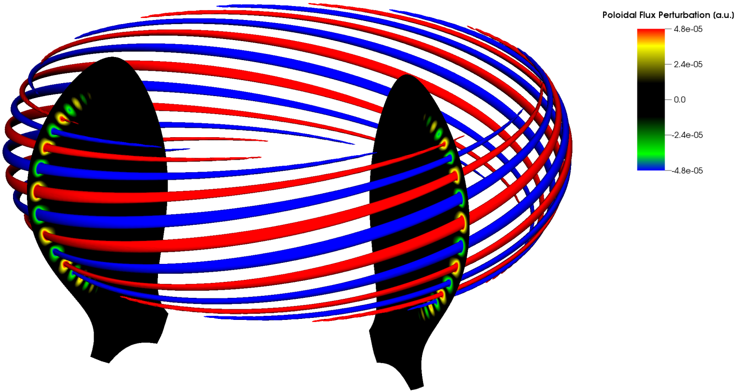


$n = 0, 8, 16$

- Red/blue surfaces correspond to 70 percent of maximum/minimum values

# Poloidal Flux Perturbation

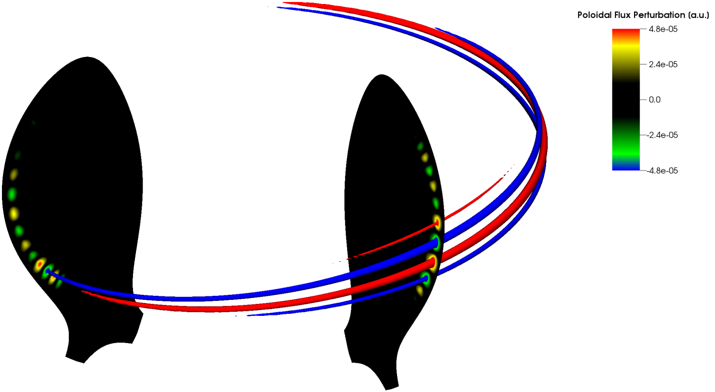


$n = 0, 1, 2, 3, 4, \ldots, 16$

- Red/blue surfaces correspond to 70 percent of maximum/minimum values
- Perturbation localized due to several strong modes with adjacent $n$

$\sim$ Solitary Magnetic Perturbations in ASDEX Upgrade Wenninger et al. [2012]

# Edge Localized Mode Simulations

## Position of Perturbations

- Radial perturbation positions differ between variables

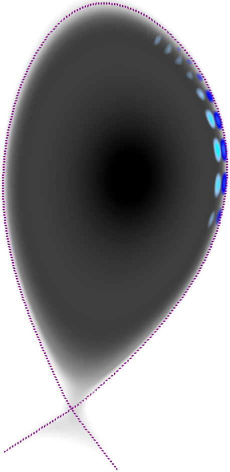

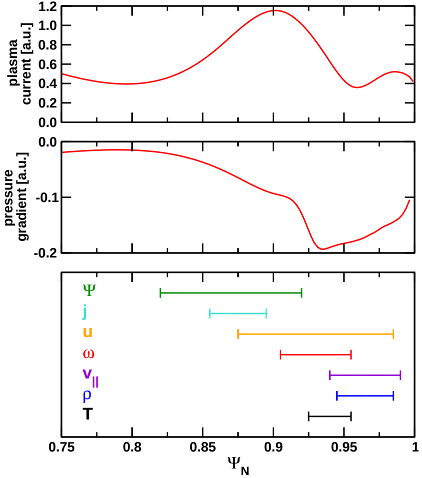

# Energy Timetraces

- Starting from small random perturbation
- Ballooning-like mode evolves, grows exponentially
- $n = 1$ driven non-linearly to large amplitude
- (Subdominant modes not shown for clarity)

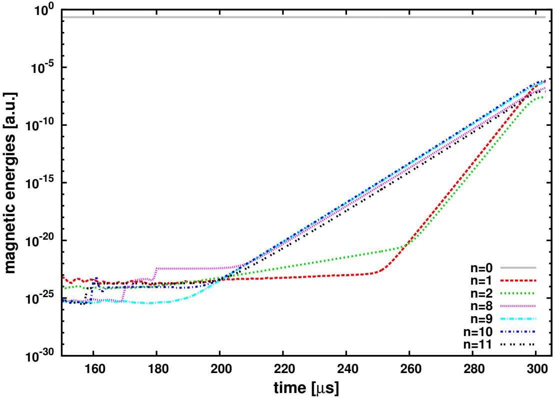

# Mode Interaction

- Consider a simpler case with $n = 0, 4, 8, 12, 16$
- Can we reproduce and understand this with a simple model?

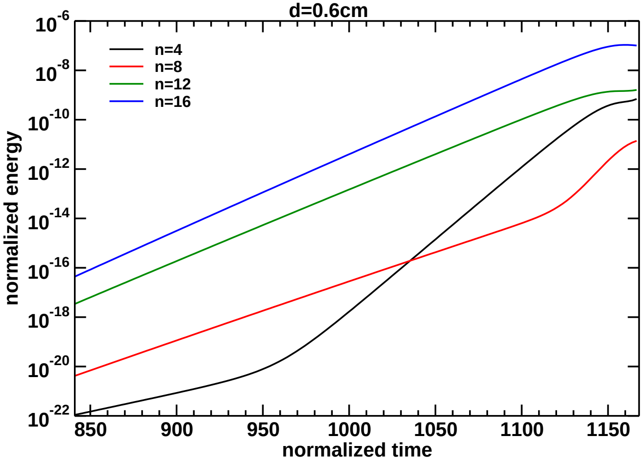

# Mode Interaction (2)

- Non-linear terms lead to mixing of toroidal modes
- Quadratic: $(n_1, n_2) \leftrightarrow n_1 \pm n_2$
- For instance: $n = 4$ coupled to $(8, 4)$, $(12, 8)$, and $(16, 12)$

# Mode Interaction (2)

- Non-linear terms lead to mixing of toroidal modes
- Quadratic: $(n_1, n_2) \leftrightarrow n_1 \pm n_2$
- For instance: $n = 4$ coupled to $(8, 4)$, $(12, 8)$, and $(16, 12)$
- Simple model (Mode rigidity, $n = 0$ fixed):

$$\dot{A}_4 = \overbrace{\gamma_4 \; A_4}^{\text{linear}} + \overbrace{\gamma_{8,-4} \; A_8 \; A_4 + \gamma_{12,-8} \; A_{12} \; A_8 + \gamma_{16,-12} \; A_{16} \; A_{12}}^{\text{non-linear interaction}}$$

# Mode Interaction (2)

- Non-linear terms lead to mixing of toroidal modes
- Quadratic: $(n_1, n_2) \leftrightarrow n_1 \pm n_2$
- For instance: $n = 4$ coupled to $(8, 4)$, $(12, 8)$, and $(16, 12)$
- Simple model (Mode rigidity, $n = 0$ fixed):

$$
\begin{aligned}
\dot{A}_4 &= \overbrace{\gamma_4 \; A_4}^{\text{linear}} + \overbrace{\gamma_{8,-4} \; A_8 \; A_4 + \gamma_{12,-8} \; A_{12} \; A_8 + \gamma_{16,-12} \; A_{16} \; A_{12}}^{\text{non-linear interaction}} \\
\dot{A}_8 &= \gamma_8 \; A_8 + \gamma_{4,4} A_4 \; A_4 + \gamma_{12,-4} A_{12} \; A_4 + \gamma_{16,-8} \; A_{16} \; A_8 \\
\dot{A}_{12} &= \gamma_{12} \; A_{12} + \gamma_{4,8} \; A_4 \; A_8 + \gamma_{16,-4} \; A_{16} \; A_4 \\
\dot{A}_{16} &= \gamma_{16} \; A_{16} + \gamma_{8,8} \; A_8 \; A_8 + \gamma_{4,12} \; A_4 \; A_{12}
\end{aligned}
$$

- Linear growth rates taken from JOREK simulation
- Energy conservation $\Rightarrow$ Six remaining free parameters $\gamma_{i,j}$
- Determine free parameters numerically by minimizing quadratic difference

# Mode Interaction (3)

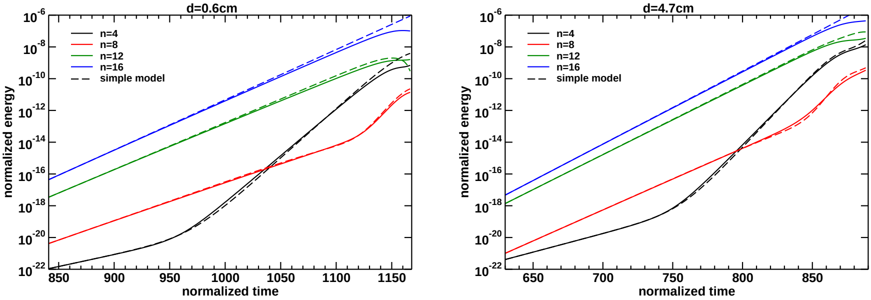


- Saturation not covered by the model (of course)
- Same set of interaction-parameters $\gamma_{i,j}$ for both wall-distances
- Non-linear growth of $n = 4$ described well: Interaction of $n = 12$ and $n = 16$
- Same mechanism brings up $n = 1$ in the simulations shown before with poloidally and toroidally localized ELMs!

# Saturation

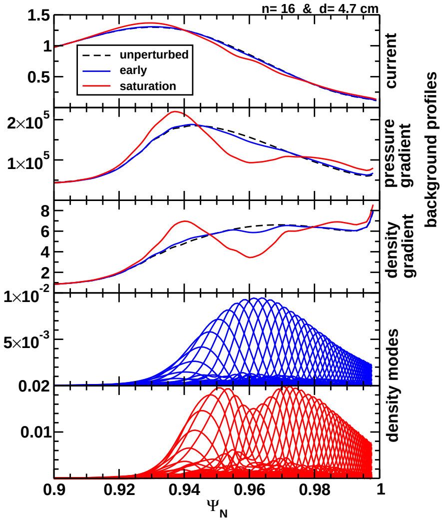


Saturation mechanisms:

- Displacement $\xi$ gets significant compared to wall distance
- Modification of background profiles by the instability

# Summary for this Part

- ELM simulations for realistic ASDEX Upgrade conditions
- Poloidal and toroidal localization of ELM-crash – similar to experiment (requires strong modes with adjacent $n$)
- Radial perturbation positions of kinetic and magnetic quantities differ
- $n = 1$ grows non-linearly – similar to experiment (requires strong modes with adjacent $n$)
- Can be explained by non-linear mode-interaction picture
- Saturation mechanisms
- Published in Hölzl et al. [2012a] and to be published in Krebs et al. [2013]

# Overview

## Physics: Growing or rotating instability

⇒ Time-dependent magnetic perturbation outside the plasma

⇒ Mirror currents in conducting structures

⇒ Changes linear and non-linear behaviour of instability

- For instance, external kink ($\sim \mu s$)
  - With close-fitting ideal wall: Fully stabilized
  - With resistive wall: Becomes a Resistive wall mode ($\sim ms$)
  - May be stabilized by active feedback-system
- Aim: Non-linear resistive wall simulations with JOREK

## Implementation

- Coupling to STARWALL (described a bit later)
- Showing status of implementation and benchmarking

# Natural boundary condition

- Current definition equation $j = \Delta^* \Psi$ in weak form (test function $v^*$):

$$\int dV \, \frac{v^*}{R^2} \, j - \int dV \, v^* \, \nabla \cdot \left( \frac{1}{R^2} \nabla \Psi \right) = 0$$

- Partial integration:

$$\int dV \, \frac{v^*}{R^2} \, j + \int dV \, \frac{1}{R^2} \, \nabla v^* \cdot \nabla \Psi - \oint dA \, \frac{v^*}{R} \, \underbrace{(\nabla \Psi \cdot \hat{\mathbf{n}} / R)}_{\equiv B_{\mathtt{tan}}} = 0.$$

- Ideal-wall boundary conditions: Boundary integral vanishes in “old” JOREK
- Natural boundary condition: Replace $B_{\mathtt{tan}}$ by STARWALL response

# STARWALL response

- STARWALL Merkel and Sempf [2006]; Strumberger et al. [2011]
  - Solves vacuum field equation outside JOREK domain (Neumann problem)
  - Resistive wall represented by triangles
  - Wall currents described by current potentials $Y_k$ at triangle nodes
  - Response matrices: $\hat{M}^{\text{id}}$
- Ideal wall (algebraic expression):

$$B_{\text{tan}} = \sum_i b_i \sum_j \hat{M}^{\text{id}}_{i,j} \, \Psi_j$$

# STARWALL response

- STARWALL Merkel and Sempf [2006]; Strumberger et al. [2011]
  - Solves vacuum field equation outside JOREK domain (Neumann problem)
  - Resistive wall represented by triangles
  - Wall currents described by current potentials $Y_k$ at triangle nodes
  - Response matrices: $\hat{M}^{\text{id}}$, $\hat{M}^{\text{ee}}$, $\hat{M}^{\text{ey}}$, $\hat{M}^{\text{ye}}$, $\hat{M}^{\text{yy}}$
- Ideal wall (algebraic expression):

$$B_{\text{tan}} = \sum_i b_i \sum_j \hat{M}^{\text{id}}_{i,j}\, \Psi_j$$

- Resistive wall:

$$B_{\text{tan}} = \sum_i b_i \left( \sum_j \hat{M}^{\text{ee}}_{i,j}\, \Psi_j + \sum_k \hat{M}^{\text{ey}}_{i,k}\, Y_k \right)$$

$$\dot{Y}_k = -\frac{\eta_w}{d_w}\, \hat{M}^{\text{yy}}_{k,k}\, Y_k - \sum_j \hat{M}^{\text{ye}}_{k,j}\, \dot{\Psi}_j$$

# Time Discretization

- Discretize wall-current evolution consistent with other JOREK equations where $Y_k^{n+1} = Y_k^n + \delta Y_k^n$:

$$(1+\xi)\left[\delta Y_k^n + \sum_j \hat{M}_{k,j}^{ye}\,\delta\Psi_j^n\right] + \Delta t\,\theta\,\frac{\eta_w}{d_w}\,\hat{M}_{k,k}^{yy}\,\delta Y_k^n$$

$$= -\Delta t\,\frac{\eta_w}{d_w}\,\hat{M}_{k,k}^{yy}\,Y_k^n + \xi\left[\delta Y_k^{n-1} + \sum_j \hat{M}_{k,j}^{ye}\,\delta\Psi_j^{n-1}\right]$$

- Solve for $\delta Y_k^n$ and insert into $B_{tan}$ at time-step $n+1$:

$$B_{tan}^{n+1} = \sum_i b_i\left[\sum_j \hat{M}_{i,j}^{ee}\cdot\left(\Psi_j^n + \delta\Psi_j^n\right) + \sum_k \hat{M}_{i,k}^{ey}\cdot\left(Y_k^n + \delta Y_k^n\right)\right]$$

- Plug result into boundary integral $\oint dA\,\frac{j_i^*}{R}\,\underbrace{\left(\nabla\Psi\cdot\hat{\mathbf{n}}/R\right)}_{\equiv B_{tan}}$

# Get this correct in Bezier formulation...

$$\sum_{i_{\text{elem}}} \int \frac{dV}{R^2} \left( j_i^* \, \delta j^n + \nabla j_i^* \cdot \nabla \delta \Psi^n \right) - \sum_{i_{\text{bnd}}} \oint dA \frac{j_i^*}{R} \sum_i b_i \sum_j \hat{E}_{i,j} \, \delta \Psi_j^n$$

$$= - \sum_{i_{\text{elem}}} \int \frac{dV}{R^2} \left( j_i^* \, j^n + \nabla j_i^* \cdot \nabla \Psi^n \right)$$

$$+ \sum_{i_{\text{bnd}}} \oint dA \frac{j_i^*}{R} \sum_i b_i \left[ \sum_k \left( \hat{F}_{i,k} \, Y_k^n + \hat{G}_{i,k} \, \delta Y_k^{n-1} \right) + \sum_j \left( \hat{H}_{i,j} \, \Psi_j^n + \hat{J}_{i,j} \, \delta \Psi_j^{n-1} \right) \right]$$

and

$$Y_k^{n+1} = Y_k^n + \sum_j \hat{A}_{k,j} \, \delta \Psi_j^n + \hat{B}_{k,k} \, Y_k^n + \hat{C}_{k,k} \, \delta Y_k^{n-1} + \sum_j \hat{D}_{k,j} \, \delta \Psi_j^{n-1}$$

where

$$\hat{S}_{k,k} = 1 + \xi + \Delta t \theta \frac{\eta w}{dw} \hat{M}^{yy}_{k,k} \qquad \hat{D}_{k,j} = \xi \hat{M}^{ye}_{k,j} / \hat{S}_{k,k} \qquad \hat{H}_{i,j} = \hat{M}^{ee}_{i,j}$$

$$\hat{A}_{k,j} = -(1+\xi) \, \hat{M}^{ye}_{k,j} / \hat{S}_{k,k} \qquad \hat{E}_{i,j} = \hat{M}^{ee}_{i,j} + \textstyle\sum_k \hat{M}^{ey}_{i,k} \, \hat{A}_{k,j} \qquad \hat{J}_{i,j} = \textstyle\sum_k \hat{M}^{ey}_{i,k} \, \hat{D}_{k,j}$$

$$\hat{B}_{k,k} = -\Delta t \frac{\eta w}{dw} \hat{M}^{yy}_{k,k} / \hat{S}_{k,k} \qquad \hat{F}_{i,k} = \hat{M}^{ey}_{i,k} \left( 1 + \hat{B}_{k,k} \right)$$

$$\hat{C}_{k,k} = \xi / \hat{S}_{k,k} \qquad \hat{G}_{i,k} = \hat{M}^{ey}_{i,k} \, \hat{C}_{k,k}$$

and

$$\int dV = \sum_{i_{\text{elem}}} \int ds \, dt \, d\phi \, J_2 \, R \qquad \oint dA = \sum_{i_{\text{bnd}}} \int dt \, d\phi \, R \sqrt{\left( \frac{\partial R}{\partial t} \right)^2 + \left( \frac{\partial Z}{\partial t} \right)^2}$$

# Freeboundary Equilibrium

- Same boundary-integral in Grad-Shafranov equation
- Allows to test parts (no time-evolution, no wall-currents)
- ITER-like limiter case as first test

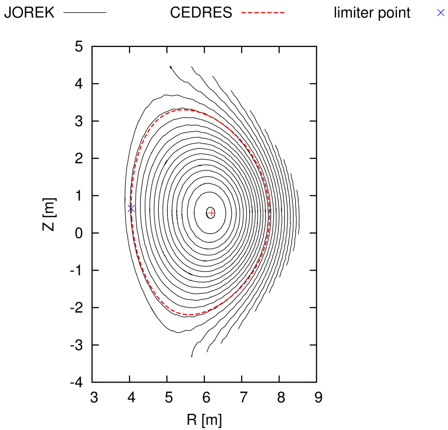


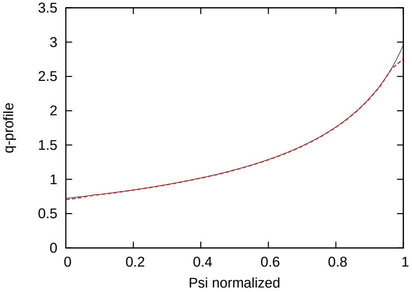


- Flux-surfaces and q-profile agree very well with CEDRES++

# Tearing Mode

- 2/1 tearing mode in a circular plasma ($R = 10$, $a = 1$)
- Concentric ideally conducting wall
- Linear growth rates:

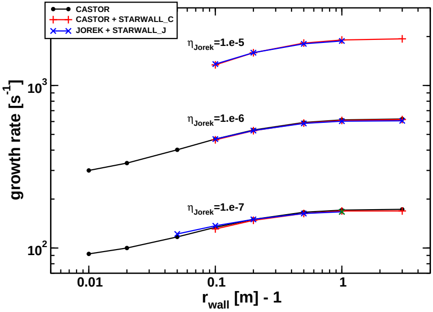


- Excellent agreement with linear CASTOR code for a variety of plasma resistivities and wall distances
- Resistive wall with zero resistivity is consistent

# Resistive Wall Mode

- 2/1 resistive wall mode in circular plasma ($R = 10$, $a = 1$)
- Concentric resistive wall
- To be compared to analytical theory and linear simulations...

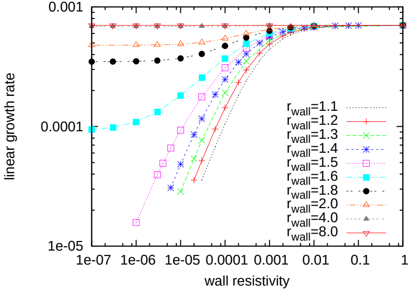


Linear growth rates for different wall radii and wall resistivities

# Resistive Wall Mode

- 2/1 resistive wall mode in circular plasma ($R = 10$, $a = 1$)
- Concentric resistive wall
- To be compared to analytical theory and linear simulations...

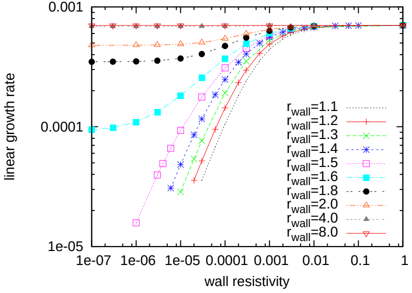


Linear growth rates for different wall radii and wall resistivities

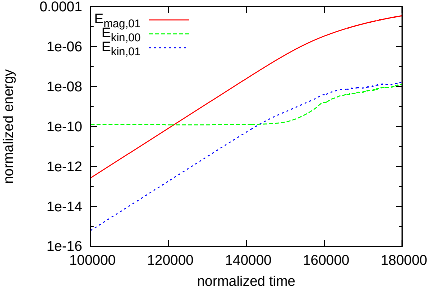


Example for non-linear saturation (stable, small time-steps required)

# Summary for this Part

- Plasma instabilities induce mirror currents in conducting structures
- These act back onto the instabilities affecting linear and non-linear behaviour
- Aim: Non-linear investigations
- Coupling JOREK and STARWALL via natural boundary condition
- Full-implicitness of JOREK time-integration is kept
- First tests:
  - Free-boundary equilibrium
  - Tearing mode with ideal wall
  - Resistive wall mode
- Described in Hölzl et al. [2012b]

# Spatial Discretization

- Toroidal Fourier-decomposition
- 2D Bezier finite elements Czarny and Huysmans [2008]
  - Bicubic Bezier surfaces: 3rd order Bernstein polynomials
  - $C^0$ and $C^1$ continuity reduces degrees of freedom per node
  - Isoparametric formulation $\rightarrow$ alignment to flux-surfaces
  - Allows for local refinement

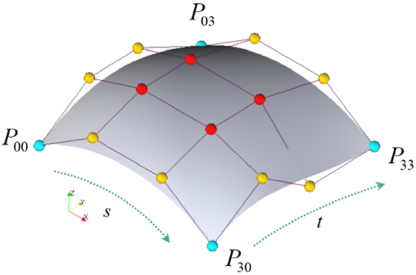


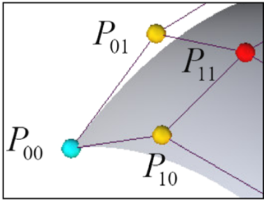


- Remaining problems:
  - Fourier basis-functions non-local
  - Problems at axis and X-point (not $C^1$)
  - Positivity not guaranteed

# Time evolution: Fully implicit

- Set of equations for variables $\mathbf{u}$:

$$\dot{\mathbf{A}}(\mathbf{u}(t)) = \mathbf{B}(\mathbf{u}(t))$$

- Time-Discretization ($\mathbf{u}^{n+1} = \mathbf{u}^n + \delta\mathbf{u}^n$):

$$\left[(1+\xi)\left(\frac{\partial \mathbf{A}}{\partial \mathbf{u}}\right)^n - \Delta t\theta\left(\frac{\partial \mathbf{B}}{\partial \mathbf{u}}\right)^n\right]\delta\mathbf{u}^n = \Delta t\ \mathbf{B}^n + \xi\left(\frac{\partial \mathbf{A}}{\partial \mathbf{u}}\right)^{n-1}\delta\mathbf{u}^{n-1}$$

  - Already involves a linearization
    (can be understood as a Newton iteration stopped after one step)
  - Crank-Nicholson: $\theta = 0.5$, $\xi = 0$ or Gears: $\theta = 1$, $\xi = 0.5$

$\Rightarrow$ Large sparse system of equations $\hat{M}\ \mathbf{x} = \mathbf{b}$

# Time evolution: GMRES and preconditioning

## Generalized Minimum Residual Method (GMRES)

- $\hat{\mathrm{M}}\ \mathbf{x} = \mathbf{b}$ solved iteratively with GMRES
- Implementation by CERFACS (France) used which requests the following operations via reverse communication (“black box”):
  - Matrix-vector product $\rightarrow$ BLAS with OpenMP parallelization
  - Dot-product between two vectors $\rightarrow$ BLAS
  - Calculation of $\mathbf{f} = \hat{\mathrm{P}}^{-1}\mathbf{g}$ for some vector $\mathbf{g}$,
    where $\hat{\mathrm{P}}$ is the left preconditioning matrix

# Time evolution: GMRES and preconditioning

## Generalized Minimum Residual Method (GMRES)

- $\hat{\mathrm{M}}\ \mathbf{x} = \mathbf{b}$ solved iteratively with GMRES
- Implementation by CERFACS (France) used which requests the following operations via reverse communication (“black box”):
  - Matrix-vector product $\rightarrow$ BLAS with OpenMP parallelization
  - Dot-product between two vectors $\rightarrow$ BLAS
  - Calculation of $\mathbf{f} = \hat{\mathrm{P}}^{-1}\mathbf{g}$ for some vector $\mathbf{g}$, where $\hat{\mathrm{P}}$ is the left preconditioning matrix

## Left Preconditioning

- Need to solve $\hat{\mathrm{P}}\ \mathbf{f} = \mathbf{g}$
- $\hat{\mathrm{P}}$: Matrix $\hat{\mathrm{M}}$ without coupling terms between toroidal modes

$\Rightarrow$ Block-diagonal matrix with few large sparse blocks

- Solve decoupled block-systems with direct solver PaStiX

# Time evolution: Pros and Cons

**Pro** Implicitness

- Time step not restricted by CFL condition

$\rightarrow$ **Large time steps possible**

**Con** Convergence

- Preconditioning based on linearization

$\rightarrow$ **Inefficient at strong non-linearities**

**Con** Efficiency

- Direct solver in preconditioning

$\rightarrow$ **Limited scalability and excessive memory consumption**

**Con** Implementation

- Derivatives of physical equations implemented (Jacobian)
- Mixed with spatial and temporal discretization

$\rightarrow$ **Hard to verify and extend**

# Time evolution: What to change?

## Four Levels:

Loop over timesteps

Linearization $\rightarrow$ **Newton-iterations?**

GMRES $\rightarrow$ **Jacobian-free?**

Preconditioner $\rightarrow$ **Matrix-free method?**

## Other possibilities

- Optimize GMRES (convergence criterion, restarts)?
- Better preconditioning for strong non-linearity?
- Improve toroidal/poloidal finite elements?
- Split into explicit and implicit parts?

# References

G.T.A. Huysmans and O. Czarny. Mhd stability in x-point geometry: simulation of elms. *Nuclear Fusion*, 47(7):659, 2007.

G. Latu, M. Becoulet, G. Dif-pradalier, V. Gradgirard, M. Hoelzl, G. Huysmans, X. Lacoste, E. Nardon, F. Orain, C. Passeron, P. Ramet, and A. Ratnani. Non-regression testing for the JOREK code, project team BACCHUS, report 8090, in preparation. Technical report, 2012.

R.P. Wenninger, H. Zohm, J.E. Boom, A. Burckhart, M.G. Dunne, R. Dux, T. Eich, R. Fischer, C. Fuchs, M. Garcia-Munoz, V. Igochine, M. Hölzl, N.C. Luhmann Jr, T. Lunt, M. Maraschek, H.W. Mueller, H.K. Park, P.A. Schneider, F. Sommer, W. Suttrop, E. Viezzer, and ASDEX Upgrade Team. Solitary magnetic perturbations at the ELM onset. *Nuclear Fusion*, 42:114025, 2012. URL `preprintathttp://arxiv.org/abs/1202.3603`.

M. Hölzl, S. Günter, R. P. Wenninger, W.-C. Muller, G. T. A. Huysmans, K. Lackner, and I. Krebs ASDEX Upgrade Team. Reduced-magnetohydrodynamic simulations of toroidally and poloidally localized edge localized modes. *Physics of Plasmas*, 19(8):082505, 2012a.

I. Krebs, M. Hölzl, and K. Lackner. to be published, 2013.

P. Merkel and M. Sempf. Feedback stabilization of resistive wall modes in the presence of multiply-connected wall structures. In *Proceedings of the 21st IAEA Fusion Energy Conference*, Chengdu, China, 2006. URL `www-naweb.iaea.org/napc/physics/FEC/FEC2006/papers/th_p3-8.pdf`. TH/P3-8.

E. Strumberger, P. Merkel, C. Tichmann, , and S. Günter. Linear stability studies in the presence of 3d wall structures. In *Proceedings of the 38th EPS Conference on Plasma Physics*, Strasbourg, France, 2011. URL `http://ocs.ciemat.es/EPS2011PAP/pdf/P5.082.pdf`. P5.082.

M. Hölzl, P. Merkel, G.T.A. Huysmans, E. Nardon, E. Strumberger, R. McAdams, I. Chapman, S. Günter, and K. Lackner. Coupling jorek and starwall codes for non-linear resistive-wall simulations. *Journal of Physics: Conference Series*, 401:012010, 2012b.

Olivier Czarny and Guido Huysmans. Bezier surfaces and finite elements for mhd simulations. *Journal of Computational Physics*, 227(16):7423 – 7445, 2008. ISSN 0021-9991. URL `http://www.sciencedirect.com/science/article/pii/S0021999108002118`.

see also: www.ipp.mpg.de/$\sim$mhoelzl

# Contributions from

P. Merkel

I. Krebs

R. Wenninger

G. Huysmans

E. Nardon

S. Günter

K. Lackner

W.-C. Müller

E. Strumberger

$$
\begin{aligned}
\frac{\partial p}{\partial t} &= -\mathbf{v} \cdot \nabla p - \gamma p \nabla \cdot \mathbf{v} + \text{Diffusion} + \text{Source} \\
\frac{\partial (\rho T)}{\partial t} &= -\mathbf{v} \cdot \nabla (\rho T) - \gamma \rho T \nabla \cdot \mathbf{v} + \nabla \cdot \left( K_\perp \nabla_\perp T + K_{||} \nabla_{||} T \right) + S_T
\end{aligned}
$$